Detection of Mooring Line Failure using Dynamic Hypothesis Testing[☆]

Vahid Hassani[a,b,*], António M. Pascoal[c], Asgeir J. Sørensen[a]

[a] *Centre for autonomous marine operations and systems (AMOS) and Dept. of Marine Technology, Norwegian Univ. of Science and Technology, Trondheim, Norway.*
[b] *SINTEF Ocean, formerly Known as Norwegian Marine Technology Research Institute (MARINTEK), Trondheim, Norway.*
[c] *Institute for Systems and Robotics (ISR/IST), LARSyS, Instituto Superior Técnico, Univ. Lisboa, Portugal.*

Abstract

This article proposes a novel methodology for the detection of mooring line breakage in thruster assisted position mooring (PM) systems, when no measurements of the tensions on the mooring lines are available. For dynamic positioning (DP) of marine vessels moored to the seabed via a turret-based spread mooring system, the thrusters provide only complementary assistance to the mooring system, which is responsible for a large part of the forces and moments required for station keeping. However, in extreme weather conditions thruster assistance is essential to avoid mooring line failure. Once a mooring line is parted, the remaining lines face an increase in the tension forces due as a means to compensate for the lost tension in the ruptured line. This in turn may lead to a cascade breakage of the mooring lines. Hence, it is of paramount importance to detect any line breakage as soon as it occurs to compensate for the lost tension by proper use of DP thruster assistance. As a contribution to solving this problem, in this paper we propose a methodology that builds on Dynamic Hypothesis Testing (DHT) whereby a set of hypotheses are assessed, at each sampling time, using the measured inputs and outputs of the thruster assisted position mooring system. While the first hypothesis corresponds to the assumption that all mooring lines are intact, the remaining hypotheses are built assuming that a single, or multiple line breakage events have taken place. At each sampling time, the inputs and outputs to the system are used to generate the conditional probability of each hypothesis being true. These conditional probabilities are then used to evaluate which hypothesis is more probable to comply with the collected measurements. In addition, we find conditions for any pair of hypothesis being distinguishable. Numerical simulations, carried out using a high fidelity nonlinear PM simulator illustrate the efficiency of the proposed methodology.

Keywords: Mooring Line Breakage, Fault Detection, Dynamic Positioning, Position Mooring, Dynamic Hypothesis Testing.

1. Introduction

Rising world oil demand, with only limited easy-to-access oil fields, is steadily pushing offshore oil and gas exploration and exploitation activities to increasingly remote, deeper areas under extreme environmental conditions. The latter expose offshore vessels and structures used for drilling and production of oil and gas to challenging operational conditions characterized by high winds reaching hurricane-force and temperatures dropping below zero. In such severe conditions, the reliability of offshore vessels and their equipments as well as the efficacy of the corresponding monitoring and control systems are fundamental to the safety and success of the operations. Some of the commercially attractive alternatives to permanent platforms for offshore oil and gas exploitation are dynamic positioning (DP) and Position Mooring (PM) systems. The research and development of thruster assisted position mooring systems follows the rich and by now mature applications of DP systems.

DP systems have been commercially available since the late 1960s for offshore drilling applications. Early DP systems were built around PID controllers driven by output measurements that were filtered using a cascade of notch and low pass filters aimed at suppressing thruster wear and tear caused by wave-induced motions. However, since notch filters introduce some phase lag around the crossover frequency, phase margin reduction and deterioration of the system performance were inevitable. To overcome this problem, PID controllers were replaced by more advanced control techniques based on optimal and Linear-Quadratic-Gaussian (LQG) control, and Kalman filter theory in Balchen et al. (1976) that were further modified and extended in Grimble et al. (1979, 1980); Balchen et al. (1980); Fung & Grimble (1983); Sælid et al. (1983); Sørensen et al. (1996); Fossen et al. (1996) and Fossen & Perez (2009a). Since the application of LQG to DP systems involved the linearization of the veseel's kinematic and dynamic equations over different operating points and the tuning of design variables such as the covariances of process and sensor noises, simpler frameworks were developed using integrator back stepping

[☆] This work was supported in part by FCT [UID/EEA/50009/2013] and the European Commission under the H2020-ICT-2014 WiMUST Project (Grant Agreement No. 645141) and was result of a collaborative effort of ISR/IST and AMOS; the Norwegian Research Council is acknowledged as the main sponsor of AMOS.

[*] Corresponding author.
Email addresses: vahid.hassani@ntnu.no (Vahid Hassani), antonio@isr.ist.utl.pt (António M. Pascoal), asgeir.sorensen@ntnu.no (Asgeir J. Sørensen)

VOR available in Ocean Engineering, Volume 159, 1 July 2018, Pages 496-503 - https://doi.org/10.1016/j.oceaneng.2018.01.021

techniques in Aarset et al. (1998); Fossen & Grøvlen (1998); Robertsson & Johansson (1998) and passive observers and nonlinear multivariate PID controllers in Fossen & Strand (1999); Strand & Fossen (1999); Strand (1999); Torsetnes et al. (2004); Fossen (2000). In recent years other techniques such as gain-scheduling Torsetnes et al. (2004), robust control Hassani et al. (2012a,b, 2017), adaptive control Tannuri et al. (2006); Hassani et al. (2010, 2013b) and hybrid control Nguyen et al. (2007b); Hassani et al. (2013b) have come to the fore. The literature on modeling and simulation of DP systems and the application of different control techniques to the design of DP controllers is vast and defies a simple summary. The reader is referred to Sørensen (2005, 2011b); Hassani et al. (2013a) and the references therein for a short presentation of the subject and its historical evolution.

PM systems have been available since the late 1980s. While PM systems are built upon DP systems, there are some key differences between the two. Namely, the main function of thruster assistance in PM systems is to keep the heading angle at a desired value and add damping in the surge, sway and yaw motions while the mooring lines keep the position of the vessel in a predefined admissible region, see Strand (1999). This strategy leads to reduced activity of the thrusters in normal environmental condition; however, in harsh environmental conditions thruster assistance helps keeping the vessel in a predefined tolerable region in order to prevent the mooring line tension from rising above safety limits. A mathematical model of a thruster assisted mooring system and a mooring line were developed in Strand et al. (1998b) and Aamo & Fossen (2000), respectively. Back stepping techniques were applied to PM systems in Strand et al. (1998a); Chen et al. (2013). In Aamo & Fossen (1999) a dynamic line tensioning controller was developed to reject constant or slowly varying environmental disturbances, and hence, reduce the thruster force and consumed fuel. In Sørensen et al. (1999) a nonlinear multivariable controller and a passivity based observer were applied to an FPSO with PM systems. A switching controller algorithm was proposed by Nguyen et al. (2007b) whereby the sea state is identified through power spectral density analysis of the vessel's motion and a suitable controller is automatically selected to increase the operation weather window of the PM system under study. The safety of DP and PM systems is of paramount concern in the marine industry, and hence, regulations are in place to define different levels of system redundancy, to prevent faults in equipment from causing accidents at the system level DNV (2014, 2015). Any failures in mooring lines can cause loss of position-keeping capability which, in turn, can lead to disasters on an unprecedented scale. In Strand et al. (1998b) a line break detection and compensation algorithm was coupled with an LQG based controller; then, any irregular tension measurement is monitored to detect a possible line break. Furthermore, a compensation mechanism is developed in Strand et al. (1998b), so that in case of line break detection, a feed-forward thrust in surge and sway and feed-forward momentum in yaw are applied to compensate for the lost tension, due to line break, and to alleviate the load increase in the remaining mooring lines. In order to reduce the possibility of mooring line breakage in harsh environmental conditions, a setpoint chasing algorithm was introduced in Nguyen & Sørensen (2009). A structural reliability index for integrity of the the mooring lines was proposed in Berntsen et al. (2004, 2006, 2009) where a new controller was developed to keep the probability of line failure below an acceptable level. A consistency based diagnosis technique was used to develop fault tolerant control of PM systems in Nguyen et al. (2007a) using the methodology developed in Blanke (2005); Blanke et al. (2006). A methodology to detect line breakage and loss of of a buoyancy element in mooring lines was developed in Fang & Blanke (2011); Blanke et al. (2012) based on a structure-graph approach Blanke et al. (2006). Detection of line breakage was studied in Ren et al. (2015) using a supervisory control framework Hespanha (2001).

Common to all of the above-mention methods, except for Ren et al. (2015), is the need for measuring the tension of mooring line forces which makes all these techniques susceptible to measurement noise or sensor failure. As a matter of fact, not all the mooring lines are equipped with loadcells and even when they are, it is frequently reported that loadcells do not work properly and offshore personnel have little confidence in the reported values; see Limited (2006). Furthermore, in the case of abnormal sensor reading for submerged turrets, it is laborious to figure out whether it was the the line that failed or the sensor that failed. A reported mooring line failure incident for an instrumented North Sea FPSO in Limited (2006), confirms that it took two weeks of data processing of the measured tension from the other lines to conclude that a recorded tension spike was indeed a real failure rather than an instrumentation fault.

The above circle of ideas motivates us to further develop a model based algorithm to detect any changes in the dynamic behavior of a PM system due to any breakage in mooring lines. To this end, we use the dynamic model of the PM system and calculate the conditional probabilities of any line break using input and output measurements only. We further develop a Dynamic Hypothesis Testing (DHT) algorithm that will be used for failure detection in mooring lines. The rationale for our approach is similar to Response Learning System (RLS) for Automatic Line Failure Detection, a suggestion proposed in Limited (2006). In RLS, by taking into account the expected performance in a measured weather condition, the response of the systems is analyzed to check if it is consistent with the expected performance and if not, could this change be due to change of system stiffness as a result of line failure. As pointed out in Limited (2006), doing so is a fairly complicated procedure that require further research and development and testing. However, if successful, it has the real benefit of being a relatively simple retrofit to existing installations, avoiding the need for expensive intervention work such as installing load-cells and wiring.

The main contribution of the current article is the development of a model based supervisor in which by measuring the inputs and outputs of the PM system, any mooring line failure is detected without the need for measuring the tension forces in mooring lines using load cells. To this end, a set of hypotheses are built and the conditional probability of each hypothesis is calculated in an iterative manner. Using the conditional prob-

abilities, all hypotheses are tested in parallel at each sampling time to detect any possible line failure. Furthermore, a sufficient condition for distinguishability of any pair of hypotheses is developed. In order to validate our proposed algorithm we use a high fidelity nonlinear PM simulator to run a series of numerical simulations to demonstrate the efficacy of the techniques proposed.

The structure of the paper is as follows. Section 2 proposes a representative dynamic model of a PM system. In section 3 we calculate the conditional probabilities of line breakage which is the core of the proposed DHT algorithm. In Section 4 we present the sufficient conditions for distinguishability of any pair of hypotheses. The results of numerical Monte-Carlo simulations with stochastic signals, carried out in the Marine Cybernetics Simulator, that illustrate the performance of developed line breakage detection algorithm are presented in Section 5. Conclusions and suggestions for future research are summarized in Section 6.

2. Control Plant Model of the PM Systems

In this section we start by introducing the vessel model described in Hassani & Pascoal (2015). The model admits the realization[1]

$$\dot{\xi}_\omega = A_\omega(\omega_0)\xi_\omega + E_\omega w_\omega \tag{1}$$
$$\eta_\omega = R(\psi_L)C_\omega\xi_\omega \tag{2}$$
$$\dot{b} = -T^{-1}b + E_b w_b \tag{3}$$
$$\dot{\eta}_L = R(\psi_L)\nu \tag{4}$$
$$M\dot{\nu} + D\nu = \tau_m + \tau_c + R^T(\psi_{tot})b \tag{5}$$
$$\eta_{tot} = \eta_L + \eta_\omega \tag{6}$$
$$\eta_y = \eta_{tot} + n \tag{7}$$

where (1) and (2) capture the 1st-order wave induced motion in surge, sway, and yaw; equation (3) represents the 1st-order Markov process approximating the unmodelled dynamics and the slowly varying bias forces (in surge and sway) and torques (in yaw) due to waves (2nd order wave induced loads), wind, and currents, where the latter are given in Earth fixed coordinates but expressed in body-axis. Vector $\eta_\omega \in \mathbb{R}^3$ captures the vessel's wave frequency motion due to 1st-order wave-induced disturbances, consists of wave frequency position (x_W, y_W) and wave frequency heading ψ_W of the vessel; $w_\omega \in \mathbb{R}^3$ and $w_b \in \mathbb{R}^3$ are zero mean Gaussian white noise vectors, and

$$A_\omega = \begin{bmatrix} 0_{3\times3} & I_{3\times3} \\ -\Omega_{3\times3} & -\Lambda_{3\times3} \end{bmatrix}, \qquad E_\omega = \begin{bmatrix} 0_{3\times1} \\ I_{3\times1} \end{bmatrix},$$
$$C_\omega = \begin{bmatrix} 0_{3\times3} & I_{3\times3} \end{bmatrix},$$

with

$$\Omega = \mathrm{diag}\{\omega_{01}^2, \omega_{02}^2, \omega_{03}^2\},$$
$$\Lambda = \mathrm{diag}\{2\zeta_1\omega_{01}, 2\zeta_2\omega_{02}, 2\zeta_3\omega_{03}\},$$

where ω_{0i} and ζ_i are the dominant wave frequency and relative damping ratio, respectively. Matrix $T = \mathrm{diag}(T_x, T_y, T_\psi)$ is a diagonal matrix of positive bias time constants and $E_b \in \mathbb{R}^{3\times3}$ is a diagonal scaling matrix. Vector $\eta_L \in \mathbb{R}^3$ consists of low frequency, Earth-fixed position (x_L, y_L) and low frequency heading ψ_L of the vessel relative to an Earth-fixed frame, $\nu \in \mathbb{R}^3$ represents the velocities decomposed in a vessel-fixed reference, and $R(\psi_L)$ is the standard orthogonal yaw angle rotation matrix (see Fossen (2011) for more details). Equation (5) describes the vessels's low frequency motion at low speed (see Fossen (2011)), where $M \in \mathbb{R}^{3\times3}$ is the generalized system inertia matrix including zero frequency added mass components, $D \in \mathbb{R}^{3\times3}$ is the linear damping matrix, $\tau_c \in \mathbb{R}^3$ is a control vector of generalized forces generated by the propulsion system, which can produce surge and sway forces as well as a yaw moment, and $\tau_m \in \mathbb{R}^3$ is the generalized forces vector generated by the mooring lines. Vector $\eta_{tot} \in \mathbb{R}^3$ represents the vessel's total motion, consisting of total position (x_{tot}, y_{tot}) and total heading ψ_{tot} of the vessel. Finally, (7) represents the position and heading measurement equation, where $n \in \mathbb{R}^3$ is zero-mean Gaussian white measurement noise.

In general, a mooring system consists of a number of mooring lines that connect the vessel, directly or through a turret, to an anchor on the sea floor. The lines are composed of synthetic fiber rope, wire and chain or a combination of the three. The generalized mooring force of a spread mooring system, projected in horizontal-plane, can be formulated as

$$\tau_m = -R^T(\psi_{tot})g_{mo}(\eta_L) - d_{mo}(\nu) \tag{8}$$

where $g_{mo} \in \mathbb{R}^{3\times3}$ (and G_{mo}) is an Earth fixed restoring term and $d_{mo} \in \mathbb{R}^{3\times3}$ (and D_{mo}) is the additional damping term due to the mooring system. To calculate the nonlinear mooring line characteristics the reader is referred to Aamo & Fossen (2000); He et al. (2014) and also dedicated software programs for marine slender structures, such as RIFLEX Fylling et al. (2011). Linearizing the generalized mooring force τ_m, one can model the mooring line effects as extra damping and restoring terms in the system in the form of[2]

$$\tau_m \approx -G_{mo}R^T(\psi_{tot})\eta_L - D_{mo}\nu. \tag{9}$$

[1] We would like to highlight the difference between the dynamic model (1)-(7), in particular (2), with the ones presented in Fossen & Strand (1999); Torsetnes et al. (2004); Sørensen (2011a). The evolution of the wave frequency components of the motion in (2), are modeled as a 2nd-order linear time invariant (LTI) system, derived with Gaussian white noise, in body frame while in Fossen & Strand (1999); Torsetnes et al. (2004); Sørensen (2011a), the wave frequency components of the motion are modeled in Earth-fixed frame. From a physical point of view, it is obvious that the wave frequency motions depend on the angle between the heading of the vessel and the direction of the wave. Assuming stationary waves, one can assume that a linear approximation can be used to described wave-induced motions in the body frame. For further details on this, readers are refereed to Hassani & Pascoal (2015); Hassani et al. (2012c).

[2] see Strand et al. (1998b) for details in development of linear mooring model.

Combining 9 and the vessels dynamic model in 1-7, the equation of the motion for PM system can be represented as

$$\dot{\xi}_\omega = A_\omega(\omega_0)\xi_\omega + E_\omega w_\omega \tag{10}$$
$$\eta_\omega = R(\psi_L)C_\omega\xi_\omega \tag{11}$$
$$\dot{b} = -T^{-1}b + E_b w_b \tag{12}$$
$$\dot{\eta}_L = R(\psi_L)\nu \tag{13}$$
$$M\dot{\nu} + (D+D_{mo})\nu + G_{mo}R^T(\psi_{tot})\eta_L = \tau_c + R^T(\psi_{tot})b \tag{14}$$
$$\eta_{tot} = \eta_L + \eta_\omega \tag{15}$$
$$\eta_y = \eta_{tot} + n. \tag{16}$$

In what follows we use a number of assumptions (that are commonly adopted in the literature, see Strand (1999); Strand & Fossen (1999); Fossen (2000); Loria et al. (2000); Torsetnes et al. (2004)):

Assumption 1 Position and heading sensor noise are neglected, that is $n = 0$, since the measurement error induced by measurement noise is negligible compared to the wave-induced motion.

Assumption 2 The amplitude of the wave-induced yaw motion ψ_ω is assumed to be small, that is, less than 2-3 degrees during normal operation of the vessel and less than 5 degrees in extreme weather conditions. Hence, $R(\psi_L) \approx R(\psi_L + \psi_W)$. From Assumption 1 it follows that $R(\psi_L) \approx R(\psi_y)$, where $\psi_y \cong \psi_L + \psi_W$ denotes the measured heading.

Assumption 3 The time-derivative of the total heading $\dot{\psi}_{tot}$ is small and close to zero (low speed assumption).

We will also exploit the model property that the bias time constant in the x and y directions are equal, i.e., $T_x = T_y$.

Let us define a new coordinates of *vessel parallel coordinates* as introduced in Fossen (2011); Sørensen (2011a) and Fossen & Perez (2009a). Vessel parallel coordinates are defined in a reference frame fixed to the vessel, with axes parallel to the Earth-fixed frame. Vector $\eta_L^p \in \mathbb{R}^3$ consists of the low frequency position (x_L^p, y_L^p) and low frequency heading ψ_L^p of the vessel expressed in body coordinates, defined as

$$\eta_L^p = R^T(\psi_{tot})\eta_L. \tag{17}$$

Computing its derivative with respect to time yields

$$\dot{\eta}_L^p = \dot{R}^T(\psi_{tot})\eta_L + R^T(\psi_{tot})\dot{\eta}_L = \dot{R}^T(\psi_{tot})R(\psi_{tot})\eta_L^p + R^T(\psi_{tot})R(\psi_L)\nu \tag{18}$$

Using a Taylor series to expand $R^T(\psi_{tot})$ about ψ_L and neglecting the higher order terms, it follows that

$$R^T(\psi_{tot})R(\psi_L) \cong I + \psi_W S, \tag{19}$$

where

$$S = \begin{bmatrix} 0 & 1 & 0 \\ -1 & 0 & 0 \\ 0 & 0 & 0 \end{bmatrix}.$$

Using simple algebra we obtain

$$\dot{R}^T(\psi_{tot})R(\psi_{tot}) = \dot{\psi}_{tot}S. \tag{20}$$

From (18), (19) and (20) we conclude that

$$\dot{\eta}_L^p \approx \dot{\psi}_{tot}S\,\eta_L^p + \nu + \psi_W S\,\nu. \tag{21}$$

We now study the time evolution of the slowly varying bias forces, b, expressed in the vessel parallel coordinates, b_p, as follows:

$$b^p = R^T(\psi_{tot})b. \tag{22}$$

Clearly,

$$b = R(\psi_{tot})b^p, \tag{23}$$

and differentiating from both sides yields

$$\dot{b} = \dot{R}(\psi_{tot})b^p + R(\psi_{tot})\dot{b}^p. \tag{24}$$

Recalling (12), (23) and (24) we now have

$$\dot{R}(\psi_{tot})b^p + R(\psi_{tot})\dot{b}^p = -T^{-1}R(\psi_{tot})b^p + E_b w_b. \tag{25}$$

Reordering (25) and multiplying both sides by $R^T(\psi_{tot})$ gives

$$\dot{b}^p = -R^T(\psi_{tot})T^{-1}R(\psi_{tot})b^p - R^T(\psi_{tot})\dot{R}(\psi_{tot})b^p + R^T(\psi_{tot})E_b w_b. \tag{26}$$

Using the assumption that $T_x = T_y$, it can be checked that $R^T(\psi_{tot})T = TR^T(\psi_{tot})$; simple algebra also shows that $R^T(\psi_{tot})\dot{R}(\psi_{tot}) = -\dot{\psi}_{tot}S$.

Equation (26) can be expressed as

$$\dot{b}^p = -T^{-1}b^p + \dot{\psi}_{tot}S\,b^p + R^T(\psi_{tot})E_b w_b. \tag{27}$$

Summarizing the equations above yields

$$\dot{\xi}_\omega = A_\omega(\omega_0)\xi_\omega + E_\omega w_\omega \tag{28}$$
$$\eta_\omega = R(\psi_L)C_\omega\xi_\omega \tag{29}$$
$$\dot{b}^p = -T^{-1}b^p + \dot{\psi}_{tot}S\,b^p + R^T(\psi_{tot})E_b w_b \tag{30}$$
$$\dot{\eta}_L^p = \dot{\psi}_{tot}S\,\eta_L^p + \nu + \psi_W S\,\nu \tag{31}$$
$$M\dot{\nu} + (D + D_{mo})\nu + G_{mo}\eta_L^p = \tau_c + b^p \tag{32}$$

Moreover, using assumptions 1, 2 and 3 a linear model is obtained that is given by

$$\dot{\xi}_\omega = A_\omega(\omega_0)\xi_\omega + E_\omega w_\omega \tag{33}$$
$$\eta_\omega^b = C_\omega\xi_\omega \tag{34}$$
$$\dot{b}^p = -T^{-1}b^p + w_b^f \tag{35}$$
$$\dot{\eta}_L^p = \nu \tag{36}$$
$$M\dot{\nu} + (D + D_{mo})\nu + G_{mo}\eta_L^p = \tau_c + b^p \tag{37}$$
$$\eta_y^f = \eta_L^p + \eta_\omega^b \tag{38}$$

where η_ω^b are wave frequency components of motion in body-coordinate axis, and w_b^f and η_y^f consists of a new modified disturbance and a modified measurement defined by $w_b^f = R^T(\psi_y)E_b w_b$ and $\eta_y^f = R^T(\psi_y)\eta_y$, respectively.[3]

[3] When designing observers for wave filtering in dynamic positioning, since the controller regulates the heading of the vessel, the designer can assign a new intensity to w_b^f; however, assigning the intensity of the noise in practice requires considerable expertise.

3. Dynamic Hypothesis Testing

Before starting our discussion on DHT, we represent the equations describing the kinematics and the dynamics of the PM system in the following standard form for multiple-input-multiple-output (MIMO)

$$\dot{x}(t) = Ax(t) + Bu(t) + Lw(t), \tag{39a}$$
$$y(t) = Cx(t) + n(t), \tag{39b}$$

where $x(t) = [{\xi_\omega}^T(t) \quad b^{pT}(t) \quad {\eta_L^p}^T(t) \quad \nu^T(t)]^T \in \mathbb{R}^{15}$ denotes the state of the system, $u(t) = M^{-1}\tau_c(t) \in \mathbb{R}^3$ its control input, $y(t) = \eta_y^f(t) \in \mathbb{R}^3$ its measured noisy output, $w(t) = [{w_\omega}^T(t) \quad {w_b^f}^T(t)]^T \in \mathbb{R}^6$ an input plant disturbance that cannot be measured, and $n(t) \in \mathbb{R}^3$ is the measurement noise. The equations in (39) are simply a compact way of presenting equations in (33)-(38); $A(\omega_0, \theta_1, \theta_2)$, B, L and C are defined

$$A = \begin{bmatrix} A_\omega(\omega_0) & \boldsymbol{O} & \boldsymbol{O} & \boldsymbol{O} \\ \boldsymbol{O} & -T^{-1} & \boldsymbol{O} & \boldsymbol{O} \\ \boldsymbol{O} & \boldsymbol{O} & \boldsymbol{O} & \boldsymbol{I} \\ \boldsymbol{O} & \boldsymbol{I} & -M^{-1}G_{mo} & -M^{-1}(D+D_{mo}) \end{bmatrix} \quad B = \begin{bmatrix} \boldsymbol{O} \\ \boldsymbol{O} \\ \boldsymbol{O} \\ \boldsymbol{I} \end{bmatrix} \quad L = \begin{bmatrix} E_\omega & \boldsymbol{O} \\ \boldsymbol{O} & \boldsymbol{I} \\ \boldsymbol{O} & \boldsymbol{O} \\ \boldsymbol{O} & \boldsymbol{O} \end{bmatrix}$$
$$C = [\, C_\omega \; \boldsymbol{O} \; \boldsymbol{I} \; \boldsymbol{O} \,], \tag{40}$$

where $\boldsymbol{O}$ and $\boldsymbol{I}$ are null and identity matrices of proper dimensions. Vectors $w(t)$ and $v(t)$ are zero-mean white Gaussian signals, mutually independent with intensities $E\{w(t)w^T(\tau)\} = Q\delta(t-\tau)$ and $E\{v(t)v^T(\tau)\} = R\delta(t-\tau)$. The initial condition $x(0)$ of (39) is a Gaussian random vector with mean and covariance given by $E\{x(0)\} = 0$ and $E\{x(0)x^T(0)\} = \Sigma(0)$, respectively. Before taking the discursion a stage further, let us emphasis that the matrix A depends on D_{mo} and G_{mo}. Any mooring line break will change D_{mo} and G_{mo} which itself leads to a change in matrix A. That being said, one should expect that any changes in configuration of mooring lines, such as mooring line breakage or change of pre-tension in mooring lines, will change the dynamic behavior of the PM systems (by changes in matrix A).

In what follows, without loss of generality, we consider the case of only single line failure[4]. Let us assume the PM system consists of $N-1$ mooring lines; hence, the A matrix can take one of N possible configurations ($N-1$ possible line break configuration plus one configuration without any fault). Now we can reformulate the problem as the case of N hypotheses $\mathcal{H}_i$, $i = 1, 2, \cdot, N$ among which only one is true; let $Z(t) \equiv \{U(t), Y(t)\}$ denote the time history of the observed input and output where $Y(t) \equiv \{y(1), y(2), \cdots, y(t)\}$ and $U(t) \equiv \{u(1), u(2), \cdots, u(t)\}$. Let us take $\mathcal{H}$ as the DHT random variable which takes the value $\mathcal{H} = \mathcal{H}_i$ on the event that the hypothesis $\mathcal{H}_i$ is true. Let us further assume that probability of any hypotheses being true at $t = 0$ is equal, i.e. $Pr\{\mathcal{H} = \mathcal{H}_i\} = \frac{1}{N}$ for $i = 1, 2, \cdots, N$. In what follows, we establish an algorithm to calculate, in real time, the conditional probability of each hypothesis based on the observation vector, i.e.

$$h_i(t) := Pr\{\mathcal{H} = \mathcal{H}_i | Z(t)\} \qquad i = 1, 2, \cdots, N. \tag{41}$$

[4]The extension of the algorithm to cover any combination of mooring line failure is straightforward.

Rationally, as more measurement are available, one should become able to to calculate conditional hypothesis probabilities $h_i(t)$ with more accuracy, which in turn leads to more certainty in the choice of the true hypothesis. To calculate the conditional probability of each hypothesis in an iterative manner, we take a Bayesian approach such that at any sampling time instant, by relying on our current belief about all the hypotheses, we only study the information hidden in the most recent measurement. To this end, by using Bayes rule, it follows that

$$\begin{aligned} Pr\{\mathcal{H} = \mathcal{H}_i \big| Z(t+1)\} &= \frac{Pr\{\mathcal{H} = \mathcal{H}_i\,,\, Z(t+1)\}}{Pr\{Z(t+1)\}} \\ &= \frac{Pr\{\mathcal{H} = \mathcal{H}_i\,,\, z(t+1)\,,\, Z(t)\}}{Pr\{z(t+1)\,,\, Z(t)\}} \end{aligned} \tag{42}$$

or equivalently,

$$\begin{aligned} &Pr\{\mathcal{H} = \mathcal{H}_i \big| Z(t+1)\} \\ &= \frac{Pr\{z(t+1)\,,\, \mathcal{H} = \mathcal{H}_i | Z(t)\} Pr\{Z(t)\}}{Pr\{z(t+1) \big| Z(t)\} Pr\{Z(t)\}} \\ &= \frac{Pr\{z(t+1)\,,\, \mathcal{H} = \mathcal{H}_i \big| Z(t)\}}{Pr\{z(t+1) \big| Z(t)\}} \end{aligned} \tag{43}$$

where $z(t+1) = (u(t+1), y(t+1))$ is the most recent measurement of input and output. Applying the conditional probability theorem to the numerator of (43) yields

$$\begin{aligned} &Pr\{\mathcal{H} = \mathcal{H}_i \big| Z(t+1)\} \\ &= \frac{Pr\{z(t+1) | \mathcal{H} = \mathcal{H}_i\,,\, Z(t)\} Pr\{\mathcal{H} = \mathcal{H}_i | Z(t)\}}{Pr\{z(t+1) \big| Z(t)\}}. \end{aligned} \tag{44}$$

Furthermore, applying the total probability theorem to the denominator of (44) yields

$$\begin{aligned} &Pr\{\mathcal{H} = \mathcal{H}_i \big| Z(t+1)\} \\ &= \frac{Pr\{z(t+1) | \mathcal{H} = \mathcal{H}_i\,,\, Z(t)\} Pr\{\mathcal{H} = \mathcal{H}_i | Z(t)\}}{\int_{\mathscr{H}} Pr\{z(t+1) \big| Z(t)\,,\, \mathcal{H}\} Pr\{\mathcal{H} \big| Z(t)\}\, d\mathcal{H}}, \end{aligned} \tag{45}$$

where $\mathscr{H}$ is the sample space of the random variable $\mathcal{H}$ and since $\mathscr{H}$ represents a finite set of variable, i.e. $\mathscr{H} = \{\mathcal{H}_1, \mathcal{H}_2, \cdots, \mathcal{H}_N\}$, equation (45) reduces to

$$\begin{aligned} &Pr\{\mathcal{H} = \mathcal{H}_i \big| Z(t+1)\} \\ &= \frac{Pr\{z(t+1) | \mathcal{H} = \mathcal{H}_i\,,\, Z(t)\} Pr\{\mathcal{H} = \mathcal{H}_i | Z(t)\}}{\sum_{k=1}^{N} Pr\{z(t+1) \big| Z(t)\,,\, \mathcal{H} = \mathcal{H}_k\} Pr\{\mathcal{H} = \mathcal{H}_k \big| Z(t)\}}. \end{aligned} \tag{46}$$

Furthermore, since the control action is a deterministic signal and known to us, equation (46) can be simplified as

$$h_i(t+1) = \frac{Pr\{y(t+1) | \mathcal{H} = \mathcal{H}_i\,,\, Z(t)\}}{\sum_{k=1}^{N} Pr\{y(t+1) \big| Z(t)\,,\, \mathcal{H} = \mathcal{H}_k\} h_k(t)} h_i(t). \tag{47}$$

Before continuing our discussion on calculation of the conditional probability of each hypothesis let us highlight an important property of (47). In fact, the proposed DHT algorithm relies on its current "credence" to adaptively settle on the most

"factual" action by exploiting the information coded in the most recent measurement. The iterative nature of (47) allows us to calculate, at each sampling time, the conditional probability of each hypothesis only based on the most recent measurement and our current credence about each hypothesis, i.e. conditional probability of the hypothesis at previous sampling time. Going back to (47), to evaluate the $h_i(t+1)$ one need to calculate $Pr\{y(t+1)|\mathcal{H} = \mathcal{H}_i\,, Z(t)\}$ for $i = 1, 2, \cdots, N$. The linearity of the system (39) and the fact that the disturbance and measurement noise are Gaussian, it is straightforward to conclude that the probability density function $Pr\{y(t+1)|\mathcal{H} = \mathcal{H}_i\,, Z(t)\}$ for $i = 1, 2, \cdots, N$ is of Gaussian nature and it suffice to find its mean and covariance to evaluate the distribution. Furthermore, these quantities (mean and covariance matrix) can be iteratively calculated by the Kalman filter incorporating the assumption that $\mathcal{H} = \mathcal{H}_i$ (see Anderson & Moore (1979))[5]

$$\hat{x}_{\mathcal{H}_i}(t+1) = A_{\mathcal{H}_i}\hat{x}_{\mathcal{H}_i}(t) + Bu(t) + K_{\mathcal{H}_i}\tilde{y}_{\mathcal{H}_i}(t), \tag{48a}$$

$$\tilde{y}_{\mathcal{H}_i}(t) = y(t) - \hat{y}_{\mathcal{H}_i}(t) \tag{48b}$$

$$\hat{y}_{\mathcal{H}_i}(t) = C\hat{x}_{\mathcal{H}_i}(t), \tag{48c}$$

$$K_{\mathcal{H}_i} = \Sigma_{\mathcal{H}_i}C^T[C\Sigma_{\mathcal{H}_i}C^T + R]^{-1} \tag{48d}$$

where $\hat{x}_{\mathcal{H}_i}(t+1)$ is estimation of the state $x(t)$ based on the observation history $Z(t)$ and assuming $\mathcal{H} = \mathcal{H}_i$ (or simply $\hat{x}_{\mathcal{H}_i}(t+1) = E\{x(t+1)|\mathcal{H} = \mathcal{H}_i\,, Z(t)\}$ where $E\{\cdot\}$ denotes expected value operator); vector $\tilde{y}_{\mathcal{H}_i}(t)$ denotes the innovation vector or one-step error in predicting the output measurement vector, and $\hat{y}_{\mathcal{H}_i}(t)$ denotes the estimation of the output vector $y(t)$ based on the observation history $Z(t-1)$ and assuming $\mathcal{H} = \mathcal{H}_i$ (or simply $\hat{y}_{\mathcal{H}_i}(t) = E\{y(t)|\mathcal{H} = \mathcal{H}_i\,, Z(t-1)\}$). The Kalman filter gain is denoted by $K_{\mathcal{H}_i}$ and the one-step error covariance matrix in estimating the states, denoted by $\Sigma_{\mathcal{H}_i}$, is the solution of the discrete Riccati equation

$$\begin{aligned} 0 = &-\Sigma_{\mathcal{H}_i} + A_{\mathcal{H}_i}\Sigma_{\mathcal{H}_i}A_{\mathcal{H}_i}^T + LQL^T \\ &- A_{\mathcal{H}_i}^T\Sigma_{\mathcal{H}_i}C^T[C\Sigma_{\mathcal{H}_i}C^T + R]^{-1}C\Sigma_{\mathcal{H}_i}A_{\mathcal{H}_i}, \end{aligned} \tag{49}$$

and it is assumed that $[A_{\mathcal{H}_i}, L]$ and $[A_{\mathcal{H}_i}, C]$ for $i = 1, \ldots, N$ are controllable and observable, respectively.

It is straightforward to verify that the covariance of the output estimation vector can be found as

$$S_{\mathcal{H}_i} = C\Sigma_{\mathcal{H}_i}C^T + R, \tag{50}$$

from which, by using the Gaussian distribution for $Pr\{y(t+1)\big|Z(t)\,, \mathcal{H} = \mathcal{H}_i\}$, the conditional probability of each hypothesis in (47) reduces to

$$h_i(t+1) = \frac{\frac{e^{-\frac{1}{2}\tilde{y}_{\mathcal{H}_i}^T(t+1)S_{\mathcal{H}_i}^{-1}\tilde{y}_{\mathcal{H}_i}(t+1)}}{\sqrt{(2\pi)^3|S_{\mathcal{H}_i}|}}}{\sum_{k=1}^N h_k(t)\frac{e^{-\frac{1}{2}\tilde{y}_{\mathcal{H}_k}^T(t+1)S_{\mathcal{H}_k}^{-1}\tilde{y}_{\mathcal{H}_k}(t+1)}}{\sqrt{(2\pi)^3|S_{\mathcal{H}_k}|}}}h_i(t). \tag{51}$$

[5] For simplicity in presentation of the results, we have used the formulation for steady state Kalman Filter, however, the results are valid for time varying kalman filter.

At this stage we would like to highlight that in order to calculate the conditional probabilities of all the hypothesis in an iterative manner, we need to run N Kalman filters in parallel. Each Kalman filter incorporates one of the N hypotheses. This means that N Kalman filters are designed using the (39) for N different realization of A matrix ($N-1$ possible line break configurations plus one configuration without any fault). Having calculated the probabilities of each hypothesis being true, one can setup an automatic alarming system which follows the evolution of the conditional probabilities and raises proper alarm and inspection procedures as soon as a faulty condition is identified.

In what follows we conclude this Section by proving that the space of N hypotheses forms a finite probability space.

Theorem 1. *Suppose that the initial conditions $h_i(0)$ satisfy $h_i(0) \in (0,1)$ and $\sum_{i=1}^N h_i(0) = 1$. Then, for every $t \geq 0$ the sample space $\mathscr{H} = \{\mathcal{H}_1, \mathcal{H}_2, \ldots, \mathcal{H}_N\}$ together with the function $P : \mathscr{H} \longrightarrow \mathbb{R}^+$, where at time t the function $P(\cdot)$ is defined as $P(\mathcal{H}_i) = h_i(t)$, forms a finite probability space.*

Proof. We need to show that $\forall \mathcal{H} \in \mathscr{H}, P(\mathcal{H}) > 0$ and $\sum_{\mathcal{H}\in\mathscr{H}} P(\mathcal{H}) = 1$.
Defining $P_{sum}(t) := \sum_{i=1}^N h_i(t)$ and computing its time-evolution using (51) yields

$$\begin{aligned} P_{sum}(t+1) &= \sum_{i=1}^N \frac{\frac{e^{-\frac{1}{2}\tilde{y}_{\mathcal{H}_i}^T(t+1)S_{\mathcal{H}_i}^{-1}\tilde{y}_{\mathcal{H}_i}(t+1)}}{\sqrt{(2\pi)^3|S_{\mathcal{H}_i}|}}}{\sum_{k=1}^N h_k(t)\frac{e^{-\frac{1}{2}\tilde{y}_{\mathcal{H}_k}^T(t+1)S_{\mathcal{H}_k}^{-1}\tilde{y}_{\mathcal{H}_k}(t+1)}}{\sqrt{(2\pi)^3|S_{\mathcal{H}_k}|}}}h_i(t) \\ &= \frac{\sum_{i=1}^N h_i(t)\frac{e^{-\frac{1}{2}\tilde{y}_{\mathcal{H}_i}^T(t+1)S_{\mathcal{H}_i}^{-1}\tilde{y}_{\mathcal{H}_i}(t+1)}}{\sqrt{(2\pi)^3|S_{\mathcal{H}_i}|}}}{\sum_{k=1}^N h_k(t)\frac{e^{-\frac{1}{2}\tilde{y}_{\mathcal{H}_k}^T(t+1)S_{\mathcal{H}_k}^{-1}\tilde{y}_{\mathcal{H}_k}(t+1)}}{\sqrt{(2\pi)^3|S_{\mathcal{H}_k}|}}} = 1. \end{aligned}$$

Therefore, if $P_{sum}(0) = 1$, then $P_{sum}(t) = 1$, $\forall t \geq 0$. We now show, that if $h_i(0) > 0$, then $h_i(t) > 0$, $\forall t > 0$. From (51), if $h_i(0) > 0$, then it follows immediately that $h_i(t)$ will be always positive. □

4. Distinguishability of Hypotheses

In this Section we study under what conditions any pair of hypotheses are distinguishable from each other. More specifically, we examine the necessary condition under which the conditional probabilities of the true hypothesis converge to one. The following theorem provides conditions for convergence of the conditional probability of the true hypothesis to one.

Theorem 2. *Let $\mathcal{H}_i$ be the true hypothesis and let $\mathscr{H}^i = \{\mathcal{H}_1, \mathcal{H}_2, \cdots, \mathcal{H}_N\} \setminus \{\mathcal{H}_i\}$ be the set of all remaining hypothesis (except $\mathcal{H}_i$). Suppose that there exist positive constants n_1, t_1, and ϵ such that for all $t \geq t_1$, $n \geq n_1$, and $\mathcal{H}_j \in \mathscr{H}^i$ the*

following condition holds:

$$\frac{1}{n}\sum_{\tau=t}^{t+n-1}\left(\frac{1}{2}\tilde{y}^T_{\mathcal{H}_i}(\tau)S^{-1}_{\mathcal{H}_i}\tilde{y}_{\mathcal{H}_i}(\tau)\right)-\frac{1}{2}\ln|S_{\mathcal{H}_i}|+\epsilon$$
$$<\frac{1}{n}\sum_{\tau=t}^{t+n-1}\left(\frac{1}{2}\tilde{y}^T_{\mathcal{H}_j}(\tau)S^{-1}_{\mathcal{H}_j}\tilde{y}_{\mathcal{H}_j}(\tau)\right)-\frac{1}{2}\ln|S_{\mathcal{H}_j}| \quad (52)$$

Then, conditional probability of true hypothesis, i.e. $h_i(t)$ governed by (51) *converges to one as $t\to\infty$.*

Proof. Let us define

$$L^j_i(t)=\frac{Pr\{\mathcal{H}=\mathcal{H}_j|Z(t)\}}{Pr\{\mathcal{H}=\mathcal{H}_i|Z(t)\}}=\frac{h_j(t)}{h_i(t)};\quad \mathcal{H}_j\in\mathscr{H}^i.$$

Using (51) we obtain

$$L^j_i(t+1)=\frac{\frac{e^{-\frac{1}{2}\tilde{y}^T_{\mathcal{H}_j}(t+1)S^{-1}_{\mathcal{H}_j}\tilde{y}_{\mathcal{H}_j}(t+1)}}{\sqrt{|S_{\mathcal{H}_j}|}}}{\frac{e^{-\frac{1}{2}\tilde{y}^T_{\mathcal{H}_i}(t+1)S^{-1}_{\mathcal{H}_i}\tilde{y}_{\mathcal{H}_i}(t+1)}}{\sqrt{|S_{\mathcal{H}_i}|}}}L^j_i(t),$$

from which it follows that

$$L^j_i(t+n)=\prod_{\tau=t}^{t+n-1}\frac{\frac{e^{-\frac{1}{2}\tilde{y}^T_{\mathcal{H}_j}(\tau+1)S^{-1}_{\mathcal{H}_j}\tilde{y}_{\mathcal{H}_j}(\tau+1)}}{\sqrt{|S_{\mathcal{H}_j}|}}}{\frac{e^{-\frac{1}{2}\tilde{y}^T_{\mathcal{H}_i}(\tau+1)S^{-1}_{\mathcal{H}_i}\tilde{y}_{\mathcal{H}_i}(\tau+1)}}{\sqrt{|S_{\mathcal{H}_i}|}}}L^j_i(t). \quad (53)$$

Taking logarithms of both sides,

$$\ln\frac{L^j_i(t+n)}{L^j_i(t)}=\sum_{\tau=t}^{t+n-1}\ln\left(\frac{e^{-\frac{1}{2}\tilde{y}^T_{\mathcal{H}_j}(\tau+1)S^{-1}_{\mathcal{H}_j}\tilde{y}_{\mathcal{H}_j}(\tau+1)}}{\sqrt{|S_{\mathcal{H}_j}|}}\right)$$
$$-\sum_{\tau=t}^{t+n-1}\ln\left(\frac{e^{-\frac{1}{2}\tilde{y}^T_{\mathcal{H}_i}(\tau+1)S^{-1}_{\mathcal{H}_i}\tilde{y}_{\mathcal{H}_i}(\tau+1)}}{\sqrt{|S_{\mathcal{H}_i}|}}\right)$$
$$=-\sum_{\tau=t}^{t+n-1}\left(\frac{1}{2}\tilde{y}^T_{\mathcal{H}_j}(\tau+1)S^{-1}_{\mathcal{H}_j}\tilde{y}_{\mathcal{H}_j}(\tau+1)\right)+\frac{n}{2}\ln|S_{\mathcal{H}_j}|$$
$$+\sum_{\tau=t}^{t+n-1}\left(\frac{1}{2}\tilde{y}^T_{\mathcal{H}_i}(\tau+1)S^{-1}_{\mathcal{H}_i}\tilde{y}_{\mathcal{H}_i}(\tau+1)\right)-\frac{n}{2}\ln|S_{\mathcal{H}_i}|. \quad (54)$$

For $t\geq t_1$ and $n\geq n_1$, by applying condition (52), we can conclude that there exists a positive ϵ such that

$$\ln\frac{L^j_i(t+n)}{L^j_i(t)}<-n\epsilon \quad (55)$$

or, equivalently,

$$L^j_i(t+n)<e^{-n\epsilon}L^j_i(t), \quad (56)$$

from which, it follows that $L^j_i(t)=\frac{Pr\{\mathcal{H}=\mathcal{H}_j|Z(t)\}}{Pr\{\mathcal{H}=\mathcal{H}_i|Z(t)\}}$ converges to zero for all $\mathcal{H}_j\in\mathscr{H}^i$, as $n\to\infty$. Since the sample space $\mathscr{H}=\{\mathcal{H}_1,\mathcal{H}_2,\ldots,\mathcal{H}_N\}$ together with the defined probability function in Theorem 1 form a finite probability space, it is now straightforward to conclude that $Pr\{\mathcal{H}=\mathcal{H}_i|Z(t)\}\to 1$, and $Pr\{\mathcal{H}=\mathcal{H}_j|Z(t)\}\to 0\quad\forall\mathcal{H}_j\in\mathscr{H}^i$. □

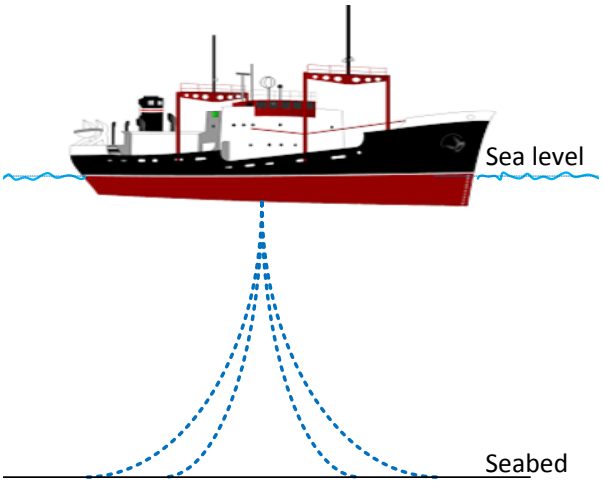

Figure 1: Graphical presentation of a vessel with the thruster assisted position mooring system.

Theorem 2 shows that as long as the condition (52) holds, any pair of hypotheses are distinguishable from each other and for sufficiently large n (number of collected measurements) the true hypothesis will be selected. Furthermore, for for Linear Time-Invariant (LTI) systems (and hence, the PM system described in (39)), the defined distinguishability condition can be verified in advance and off-line.

5. Numerical Simulations

The proposed procedure for detection of mooring line breakage is now evaluated using the Marine Cybernetics Simulator (MCSim) Sørensen et al. (2003); Perez et al. (2005, 2006) which is later enhanced to Marine System Simulator (MSS) Fossen & Perez (2009b). The MCSim is a modular multi-disciplinary simulator based on Matlab/Simulink, developed at the Norwegian University of Science and Technology (NTNU). It includes high fidelity environmental module, simulation plants and actuators models, and guidance and navigation control modules. The environmental section of MCSim contains different wave models, surface current models, and wind models. The vessel dynamics module consists of a wave frequency model and a low frequency model, based on the standard 6DOF vessel dynamics, whose inputs are the environmental loads and the interaction forces from thrusters and the external connected systems. It also captures hydrodynamic effects, generalized coriolis and centripetal forces, nonlinear damping and current forces, and generalized restoring forces. The actuation unit of MCSim, i.e. thruster and shaft module, contains thrust allocation routine for non-rotating thrusters, thruster dynamics and local thruster control. The control library contains different controllers, namely, nonlinear multivariable PID controller, for DP.

Numerical simulations for a PM system with four mooring lines, see Fig. 1, is conducted using MCSim. The vessel is excited by waves, wind, and currents and mooring lines are exposed to the ocean current disturbances. The Joint North Sea

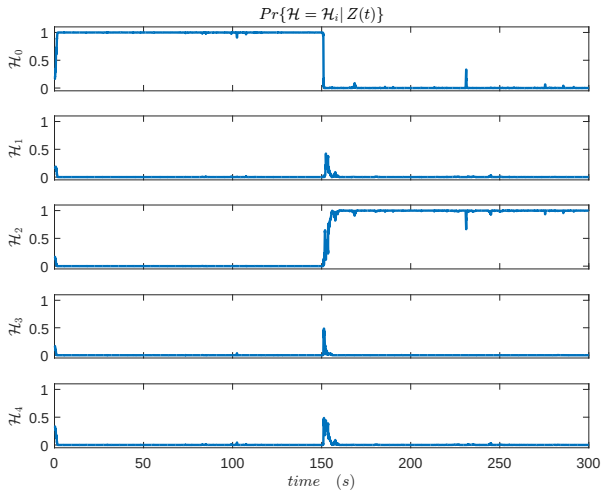

Figure 2: Time evolution of the conditional probabilities of hypothesis.

Wave Project (JONSWAP) Hasselmann et al. (1973) is used to simulate irregular waves. We construct the set of hypotheses as $\mathscr{H} = \{\mathcal{H}_0, \mathcal{H}_1, \mathcal{H}_2, \mathcal{H}_3, \mathcal{H}_4\}$ where $\mathcal{H}_0$ is the hypothesis that all the mooring lines in the PM system are intact and $\mathcal{H}_1, \cdots, \mathcal{H}_4$ denote hypotheses of mooring line $1, \cdots, 4$ breakage, respectively.

Fig. 2 presents the results of simulations where the PM system is initially moored by all four mooring lines and at $t = 150$ (sec) line number two breaks. The results show that the true hypotheses is identified in few seconds.

6. Conclusions and Future Research

This article presented and analyzed a new algorithm for detection of mooring line breakage in thruster assisted position mooring, with no tension measurement, based on iterative Dynamic Hypothesis Testing. To this end, a set of different hypotheses were formed in which one hypothesis is set up assuming that all mooring lines are intact and the rest of hypotheses are build assuming that a single, or multiple, line breakage has happened. After deriving a dynamic model of the thruster assisted position mooring system, the conditional probabilities of each hypothesis were computed in an iterative manner. It was shown that the set of the hypotheses and the calculated conditional probabilities form a finite probability space. We also studied the necessary condition under which any pair of hypotheses are distinguishable. Numerical simulation demonstrated the efficacy of the proposed methodology and confirmed that the method developed holds promise for practical applications. Application of the method developed to model test experiments is planned for near future. Another topic that warrants consideration is that of deriving the conditional probabilities of hypotheses under non-Gaussian disturbances.

References

Aamo, O. M., & Fossen, T. I. (1999). Controlling line tension in thruster assisted mooring systems. In *Control Applications, 1999. Proceedings of the 1999 IEEE International Conference on* (pp. 1104–1109). IEEE volume 2.

Aamo, O. M., & Fossen, T. I. (2000). Finite element modelling of mooring lines. *Mathematics and computers in simulation*, *53*, 415–422.

Aarset, M. F., Strand, J. P., & Fossen, T. I. (1998). Nonlinear vectorial observer backstepping with integral action and wave filtering for ships. In *Proc. the IFAC Conf. on Control Appl. in Marine Systems (CAMS98)* (pp. 83–89). Fukuoka, Japan.

Anderson, B. D. O., & Moore, J. B. (1979). *Optimal Filtering*. New Jersey, USA: Prentice-Hall.

Balchen, J., Jenssen, N. A., Mathisen, E., & Sælid, S. (1980). A dynamic positioning system based on Kalman filtering and optimal control. *Modeling, Identification and Control (MIC)*, *1*, 135–163.

Balchen, J., Jenssen, N. A., & Sælid, S. (1976). Dynamic positioning using Kalman filtering and optimal control theory. In *the IFAC/IFIP Symp. On Automation in Offshore Oil Field Operation* (pp. 183–186). Bergen, Norway.

Berntsen, P., Aamo, O., & Leira, B. (2006). Position mooring based on structural reliability. In *Proceedings of the 7th conference on manoeuvring and control of marine craft*.

Berntsen, P. I. B., Aamo, O. M., & Leira, B. J. (2009). Ensuring mooring line integrity by dynamic positioning: Controller design and experimental tests. *Automatica*, *45*, 1285–1290.

Berntsen, P. I. B., Leira, B. J., Aamo, O. M., & Sorensen, A. J. (2004). Structural reliability criteria for control of large-scale interconnected marine structures. In *ASME 2004 23rd International Conference on Offshore Mechanics and Arctic Engineering* (pp. 297–306). American Society of Mechanical Engineers.

Blanke, M. (2005). A structure-graph approach to diagnosis and control reconfiguration design-exemplified by station-keeping control. In *ASNE Symposium on Reconfiguration and Survivability*. American Society of Naval Engineers.

Blanke, M., Fang, S., Galeazzi, R., & Leira, B. J. (2012). Statistical change detection for diagnosis of buoyancy element defects on moored floating vessels. *IFAC Proceedings Volumes*, *45*, 462–467.

Blanke, M., Kinnaert, M., Lunze, J., Staroswiecki, M., & Schröder, J. (2006). *Diagnosis and fault-tolerant control* volume 691. Springer.

Chen, M., Ge, S. S., How, B. V. E., & Choo, Y. S. (2013). Robust adaptive position mooring control for marine vessels. *IEEE Transactions on Control Systems Technology*, *21*, 395–409.

DNV (2014). Dynamic positioning systems. *Rules for Classification of Ships*, (pp. 1–53).

DNV (2015). Position mooring. *OFFSHORE STANDARD DNV-OS-E301*, (pp. 1–114).

Fang, S., & Blanke, M. (2011). Fault monitoring and fault recovery control for position-moored vessels. *International Journal of Applied Mathematics and Computer Science*, *21*, 467–478.

Fossen, T. I. (2000). Nonlinear passive control and observer design for ships. *Modeling, Identification and Control (MIC)*, *21*, 129–184.

Fossen, T. I. (2011). *Handbook of Marine Craft Hydrodynamics and Motion Control*. Chichester, UK: John Wiley & Sons. Ltd.

Fossen, T. I., & Grøvlen, A. . (1998). Nonlinear output feedback control of dynamically positioned ships using vectorial observer backstepping. *IEEE Transactions on Control Systems Technology*, *6*, 121–128.

Fossen, T. I., & Perez, T. (2009a). Kalman filtering for positioning and heading control of ships and offshore rigs. *IEEE Control Systems Magazine*, *29*, 32–46.

Fossen, T. I., & Perez, T. (2009b). Marine systems simulator (MSS). "www.marinecontrol.org".

Fossen, T. I., Sagatun, S. I., & Sørensen, A. J. (1996). Identification of dynamically positioned ships. *Journal of Control Engineering Practice*, *4*, 369–376.

Fossen, T. I., & Strand, J. P. (1999). Passive nonlinear observer design for ships using lyapunov methods: Full-scale experiments with a supply vessel. *Automatica*, *35*, 3–16.

Fung, P. T.-K., & Grimble, M. J. (1983). Dynamic ship positioning using self-tuning kalman filter. *IEEE Transactions on Automatic Control*, *28*, 339–349.

Fylling, I., Larsen, C., Sødahl, N., Passano, E., Bech, A., Engseth, A., Lie, H., & Ormberg, H. (2011). RIFLEX User's Manual V3.6rev10. *MARINTEK, Trondheim, Norway*, (pp. 55–56).

Grimble, M. J., Patton, R. J., & Wise, D. A. (1979). The design of dynamic ship positioning control systems using extended Kalman filtering techniques. In *Proc. IEEE Oceans Conference (Oceans'79)* (pp. 488–497). San Diego, CA.

Grimble, M. J., Patton, R. J., & Wise, D. A. (1980). The design of dynamic ship

positioning control systems using stochastic optimal control theory. *Optimal Control Applications and Methods*, *1*, 167–202.

Hassani, V., & Pascoal, A. (2015). Wave filtering and dynamic positioning of marine vessels using a linear design model: Theory and experiments. In C. Ocampo-Martinez, & R. R. Negenborn (Eds.), *Transport of Water versus Transport over Water* (pp. 315–343). Springer International Publishing volume 58 of *Operations Research/Computer Science Interfaces Series*. URL: `http://dx.doi.org/10.1007/978-3-319-16133-4_17`. doi:`10.1007/978-3-319-16133-4_17`.

Hassani, V., Pascoal, A. M., Aguiar, A. P., & Athans, M. (2010). A multiple model adaptive wave filter for dynamic ship positioning. In *Proc. the IFAC Conf. on Control Appl. in Marine Systems (CAMS10)*. Rostock, Germany.

Hassani, V., Sørensen, A. J., & Pascoal, A. M. (2012a). Robust dynamic positioning of offshore vessels using mixed-μ synthesis, part I: Designing process. In *Proc. ACOOG'12 - IFAC Workshop on Automatic Control in Offshore Oil and Gas Production* (pp. 177–182). Trondheim, Norway.

Hassani, V., Sørensen, A. J., & Pascoal, A. M. (2012b). Robust dynamic positioning of offshore vessels using mixed-μ synthesis, part II: Simulation and experimental results. In *Proc. ACOOG'12 - IFAC Workshop on Automatic Control in Offshore Oil and Gas Production* (pp. 183–188). Trondheim, Norway.

Hassani, V., Sørensen, A. J., & Pascoal, A. M. (2013a). Adaptive wave filtering for dynamic positioning of marine vessels using maximum likelihood identification: Theory and experiments. In *Proc. of the 9th IFAC Conference on Control Applications in Marine Systems* (pp. 203–208). Elsevier volume 46.

Hassani, V., Sørensen, A. J., & Pascoal, A. M. (2013b). A novel methodology for robust dynamic positioning of marine vessels: Theory and experiments. In *Proc. of the 2013 American Control Conference* (pp. 560–565). IEEE.

Hassani, V., Sørensen, A. J., Pascoal, A. M., & Aguiar, A. P. (2012c). Developing a linear model for wave filtering and dynamic positioning. In *Proc. CONTROLO'12 - the 10th Portuguese Conference on Automatic Control* (pp. 298–303). Madeira, Portugal.

Hassani, V., Sørensen, A. J., Pascoal, A. M., & Athans, M. (2017). Robust dynamic positioning of offshore vessels using mixed-μ synthesis modeling, design, and practice. *Ocean Engineering*, *129*, 389–400.

Hasselmann, K., Barnett, T. P., Bouws, E., Carlson, H., Cartwright, D., Enke, K., Ewing, J. A., Gienapp, H., Hasselmann, D. E., Kruseman, P., Meerburg, A., Müller, P., Olbers, D. J., Richter, K., Sell, W., & Walden, H. (1973). Measurements of wind-wave growth and swell decay during the joint north sea wave project (JONSWAP). *Ergnzungsheft zur Deutschen Hydrographischen Zeitschrift Reihe*, *8*, 1–95.

He, W., Zhang, S., & Ge, S. S. (2014). Robust adaptive control of a thruster assisted position mooring system. *Automatica*, *50*, 1843–1851.

Hespanha, J. P. (2001). Tutorial on supervisory control. Lecture Notes for the workshop *Control using Logic and Switching* for the 40th Conf. on Decision and Contr., Orlando, Florida. Available at `http://www.ece.ucsb.edu/~hespanha/published`.

Limited, N. D. E. (2006). *Floating production system JIP FPS mooring integrity*. Technical Report Research report 444 prepared for the Health and Safety Executive (HSE).

Loria, A., Fossen, T. I., & Panteley, E. (2000). A separation principle for dynamic positioning of ships: theoretical and experimental results. *IEEE Trans. on Contr. Syst. and Tech.*, *8*, 332–343.

Nguyen, D. T., Blanke, M., & Sørensen, A. J. (2007a). Diagnosis and fault-tolerant control for thruster-assisted position mooring. *IFAC Proceedings Volumes*, *40*, 287–292.

Nguyen, D. T., & Sørensen, A. J. (2009). Setpoint chasing for thruster-assisted position mooring. *IEEE Journal of Oceanic Engineering*, *34*, 548–558.

Nguyen, T. D., Sørensen, A. J., & Quek, S. T. (2007b). Design of hybrid controller for dynamic positioning from calm to extreme sea conditions. *Automatica*, *43*, 768–785.

Perez, T., Smogeli, O. N., Fossen, T. I., & Sørensen, A. J. (2005). An overview of marine systems simulator (MSS): A simulink toolbox for marine control systems. In *Proc. of Scandinavian Conference on Simulation and Modeling (SIMS'05)*. Trondheim, Norway.

Perez, T., Sørensen, A. J., & Blanke, M. (2006). Marine vessel models in changing operational conditions a tutorial. In *14th IFAC Symposium on System Identification (SYSID'06)*. Newcastle, Australia.

Ren, Z., Skjetne, R., & Hassani, V. (2015). Supervisory control of line breakage for thruster-assisted position mooring system. *IFAC-PapersOnLine*, *48*, 235–240.

Robertsson, A., & Johansson, R. (1998). Comments on" nonlinear output feedback control of dynamically positioned ships using vectorial observer backstepping". *IEEE Transactions on control systems technology*, *6*, 439–441.

Sælid, S., Jenssen, N. A., & Balchen, J. (1983). Design and analysis of a dynamic positioning system based on Kalman filtering and optimal control. *IEEE Transactions on Automatic Control*, *28*, 331–339.

Sørensen, A. J. (2005). Structural issues in the design and operation of marine control systems. *Annual Reviews in Control*, *29*, 125–149.

Sørensen, A. J. (2011a). *Lecture Notes on Marine Control Systems*. Technical Report UK-11-76 Norwegian University of Science and Technology.

Sørensen, A. J. (2011b). A survey of dynamic positioning control systems. *Annual Reviews in Control*, *35*, 123–136.

Sørensen, A. J., Pedersen, E., & Smogeli, O. (2003). Simulation-based design and testing of dynamically positioned marine vessels. In *Proc. of International Conference on Marine Simulation and Ship Maneuverability (MARSIM'03)*. Kanazawa, Japan.

Sørensen, A. J., Sagatun, S. I., & Fossen, T. I. (1996). Design of a dynamic positioning system using model-based control. *Journal of Control Engineering Practice*, *4*, 359–368.

Sørensen, A. J., Strand, J. P., & Fossen, T. I. (1999). Thruster assisted position mooring system for turret-anchored fpsos. In *Control Applications, 1999. Proceedings of the 1999 IEEE International Conference on* (pp. 1110–1117). IEEE volume 2.

Strand, J. P. (1999). *Nonlinear Position Control Systems Design for Marine Vessels*. Ph.D. thesis Dept. of Eng. Cybernetics, Norwegian University of Science and Technology, Trondheim, Norway.

Strand, J. P., Ezal, K., Fossen, T. I., & Kokotovic, P. V. (1998a). Nonlinear control of ships: a locally optimal design. *Proceedings of the IFAC NOLCOS'98*, *98*, 732–738.

Strand, J. P., & Fossen, T. I. (1999). Nonlinear passive observer for ships with adaptive wave filtering. *New Directions in Nonlinear Observer Design (H. Nijmeijer and T. I. Fossen, Eds.), Springer-Verlag London Ltd.*, (pp. 113–134).

Strand, J. P., Sørensen, A. J., & Fossen, T. I. (1998b). Design of automatic thruster assisted mooring systems for ships. *Modeling, Identification and Control*, *19*, 61–75. doi:`10.4173/mic.1998.2.1`.

Tannuri, E. A., Kubota, L. K., & Pesce, C. P. (2006). Adaptive control strategy for the dynamic positioning of a shuttle tanker during offloading operations. *Journal of Offshore Mechanics and Arctic Engineering*, *128*, 203–210.

Torsetnes, G., Jouffroy, J., & Fossen, T. I. (2004). Nonlinear dynamic positioning of ships with gain-scheduled wave filtering. In *Proc. IEEE Conference on Decision and Control (CDC'04)*. Paradise Islands, The Bahamas.